Kaneva M.V., et al. *Nanosystems: Phys. Chem. Math.*, 2025, **16** (5), 706–711. http://nanojournal.ifmo.ru **DOI 10.17586/2220-8054-2025-16-5-706-711** 

# Influence of precursors variation on the morphology and electrochemical performance of $NiS_x$ thin films synthesized via the SILAR

Maria V. Kaneva $^a$ , Alexandra A. Meleshko $^b$ , Maxim I. Tenevich $^c$ , Maria O. Enikeeva $^d$ , Ilya A. Kodintsev $^e$ , Artem A. Lobinsky $^f$ 

loffe Institute, Hydrogen Energy Laboratory, St. Petersburg, Russia

 $^a$ skt94@bk.ru,  $^b$ alya\_him@mail.ru,  $^c$ mtenevich@gmail.com,  $^d$ enikeeva123@mail.ioffe.ru,  $^e$ i.a.kod@mail.ru,  $^f$ lobinski.a@mail.ru

Corresponding author: Maria V. Kaneva, skt94@bk.ru

#### PACS 81.07.Bc

ABSTRACT In this work, nickel sulfide thin films were synthesized via the SILAR method using different nickel salts as precursors. The influence of the precursor salt on the morphology and electrochemical performance of the layers was systematically investigated. SEM analysis revealed that  $NiS_x$  films prepared from nickel chloride exhibited the most uniform and crack-free morphology. Electrochemical measurements demonstrated a strong correlation between film quality and capacitive behaviour. Notably, the  $NiS_x$  electrode synthesized using nickel chloride achieved a maximum specific capacitance of 1902 F/g at a current density of 1 A/g. These findings highlight the critical role of precursor selection in optimizing the structural and electrochemical properties of nickel sulfide electrodes for energy storage applications.

KEYWORDS nickel sulfide, precursors, thin films, SILAR, electrode, supercapacitor

ACKNOWLEDGEMENTS This work was supported by Russian Science Foundation (grant number 24-19-20060, https://rscf.ru/project/24-19-20060/) and St. Petersburg Science Foundation (agreement number 24-19-20060). The authors are very grateful to Dr. Dmitry Danilovich for their invaluable research assistance of FTIR spectroscopy. FTIR and SEM studies of the samples performed using devices of the Engineering Center of the St. Petersburg State Technological Institute (Technical University).

FOR CITATION Kaneva M.V., Meleshko A.A., Tenevich M.I., Enikeeva M.O., Kodintsev I.A., Lobinsky A.A. Influence of precursors variation on the morphology and electrochemical performance of  $NiS_x$  thin films synthesized via the SILAR. *Nanosystems: Phys. Chem. Math.*, 2025, **16** (5), 706–711.

## 1. Introduction

The development of high-performance supercapacitors is crucial for advancing modern energy storage technologies aimed at supporting sustainable energy systems. Supercapacitors are widely recognized for their remarkable power density, fast charge—discharge rates, and long cycle life, which enable them to bridge the gap between conventional dielectric capacitors and rechargeable batteries. These attributes make them ideal candidates for applications ranging from electric vehicles to renewable energy integration, where high power output and rapid energy delivery are essential [1].

Among various classes of electrode materials, transition metal sulfides have emerged as particularly promising for next-generation supercapacitors due to their excellent redox activity, high electrical conductivity, and large theoretical capacitance. Compared to their oxide counterparts, sulfides provide a greater number of accessible redox-active sites and lower electronegativity, which contribute to enhanced charge storage performance and improved structural flexibility. These features allow metal sulfides to achieve higher energy and power densities, along with excellent cycling stability [2, 3].

Nickel sulfide (NiS), in particular, has attracted significant attention due to its abundance, low cost, and outstanding electrochemical properties. Various crystalline forms of nickel sulfide, such as NiS,  $Ni_3S_2$ , and  $Ni_3S_4$ , exhibit high theoretical capacitances and reversible redox behavior, making them suitable candidates for use in hybrid and pseudocapacitor systems [4,5].

To date, the synthesis of nickel sulfide nanostructures for supercapacitor applications has been primarily achieved through hydrothermal [6, 7] and solvothermal methods [8], often conducted at elevated temperatures (typically  $160 - 180\,^{\circ}$ C) and in the presence of surfactants. Other methods such as electrodeposition [9], chemical bath deposition [10], and ultrasound-assisted soaking [11] have also been reported. While these techniques can yield high-performance materials, they often require complex conditions, long synthesis times, and additional reagents.

In this work, we report a facile and surfactant-free approach for the synthesis of nickel sulfide thin films directly on nickel foam substrates using the Successive Ionic Layer Adsorption and Reaction (SILAR) method at room temperature [12–14]. The SILAR technique offers a simple, low-cost, and easily controllable route for thin film fabrication, making it a viable alternative to traditional synthesis methods.

As is known, anions of precursor salts have a significant effect on the crystallization process, nucleation, determining the rate of crystal grown, morphology and structure of the crystals formed. Changes in the concentration and nature of anions can lead to significant changes in these parameters, as evidenced by earlier in detail studies [15, 16]. However, no systematic studies have been conducted on the effect nature of the anion on the morphology of the transition metal sulfides thin films obtained via SILAR synthesis. By varying the nickel salt precursor used during deposition we systematically investigated the influence of precursor chemistry on the resulting film morphology and electrochemical behavior. Among the synthesized samples, the electrode derived from nickel chloride demonstrated the most uniform crack-free surface morphology and exhibited the highest electrochemical performance, achieving a specific capacitance of 1902 F/g at a current density of 1 A/g in 1 M KOH electrolyte. Moreover, this sample displayed excellent rate capability and stable cycling performance over 1000 charge-discharge cycles.

## 2. Experimental

#### 2.1. Synthesis of nickel sulfides on Ni foam

Aqueous solutions of nickel (II) chloride hexahydrate (NiCl<sub>2</sub>  $\times$  6H<sub>2</sub>O), nickel (II) sulfate heptahydrate (NiSO<sub>4</sub>  $\times$  7H<sub>2</sub>O), nickel (II) acetate tetrahydrate (NiAc<sub>2</sub>  $\times$  4H<sub>2</sub>O), nickel (II) nitrate hexahydrate (Ni(NO<sub>3</sub>)<sub>2</sub>  $\times$  6H<sub>2</sub>O) were used for the synthesis of nickel sulfides by SILAR as the cationic precursors. Sodium sulfide nonahydrate (Na<sub>2</sub>S  $\times$  9H<sub>2</sub>O) was used as the anion precursor. All solutions were prepared at a concentration of 0.05 M using distilled water. Nickel foam (NF) with a porosity of 110 PPI and dimensions of approximately 15  $\times$  15 mm was used as the substrate. Prior to synthesis, the NF substrates were treated with ethanol in combination with ultrasound to remove organic contaminants. To eliminate the surface oxide layer, the substrates were subsequently immersed in 6 M hydrochloric acid (HCl) for 15 minutes, rinsed thoroughly with distilled water, and dried at 60  $^{\circ}$ C in air.

In the first step of SILAR, the pretreated substrates were fixed in clamps of the automated installation, immersed for 15 s into solution of nickel salt, and then washed with distilled water to remove excess reagent. In the second step, the substrates were immersed for 15 s in the  $Na_2S$  solution and again washed in distilled water. This sequence of treatments constituted a single SILAR cycle, which was repeated 10 times. After completion of layering cycles, the substrates were dried in an air atmosphere.

#### 2.2. Materials characterizations and electrochemical measurements

The morphological characteristics of the synthesized nickel sulfide films were examined using a Tescan Vega 3 SBH scanning electron microscope (SEM). Elemental composition and surface distribution of elements were determined via energy-dispersive X-ray spectroscopy (EDX) using an Oxford Instruments INCA x-act system coupled to the SEM. FTIR transmittance spectra were recorded on Shimadzu IRTracer-100 FTIR spectrophotometer. Phase composition and crystallinity were assessed by powder X-ray diffraction (PXRD), carried out on a DRON-8H diffractometer (Russia, Bourevestnik, JSC) (Cu K $\alpha$  radiation ( $\lambda = 1.5406$  Å)). Diffraction patterns were recorded in Bragg–Brentano geometry in the  $\omega$ -2 $\theta$  scanning mode using PSD in the angle range  $2\theta = 30 - 65^{\circ}$  in increments of  $0.01^{\circ}$ . Phase identification was performed by comparing the obtained patterns with standard reference data from the PDF-2 database.

The electrochemical properties of NiS/NF as cathode of supercapacitor was investigated in standard three-electrode cell measurements with 1 M KOH electrolyte using SmartStat PS-250 (SmartStat, Russia, Chernogolovka) at room temperature. The reference and counter electrodes were an Hg/HgO and a carbon rod, respectively. Cyclic voltammetry (CV) measurements were obtained in the potential windows from 0.0 to 0.6 V (vs. Hg/HgO) at scan rates of 10 mV/s. Galvanostatic charge discharge (GCD) measurements were obtained at current densities of 1 A/g. The specific capacitance (C, F/g) of the prepared electrode was calculated from the GCD measurements using eq. (1):

$$C = \frac{It}{mV},\tag{1}$$

where I is the applied current (A), t is the discharge time (s), V is the potential window (V) and m is the mass of the electroactive material (g). The mass of the electroactive material was determined from the difference in mass between the initial substrate and the substrate with the NiS layer.

### 3. Results and discussion

In this study, we investigated the synthesis conditions of nickel sulfide (NiS) using the SILAR method, with a particular focus on the influence of different nickel salts as precursors. Specifically, nickel sulfate, nickel acetate, nickel chloride, and nickel nitrate were employed as sources of Ni<sup>2+</sup> ions. The primary objective was to examine how the nature of the nickel salt affects the morphology of the resulting nickel sulfide layers.

The SEM images and EDX spectra are shown in Fig. 1.

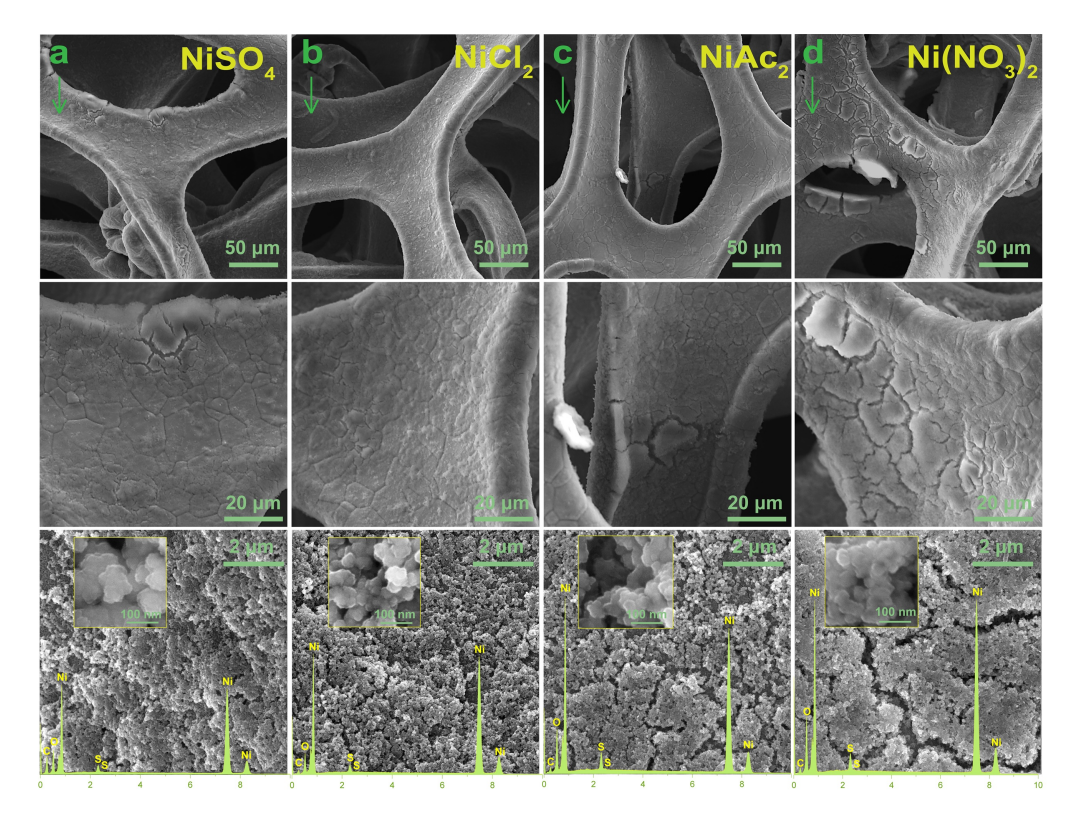


FIG. 1. SEM images and EDX spectra of nickel sulfides synthesized using NiSO<sub>4</sub>, NiCl<sub>2</sub>, NiAc<sub>2</sub> and Ni(NO<sub>3</sub>)<sub>2</sub> on NF after 10 SILAR cycles at different magnifications

Our findings reveal that the choice of precursor salt plays a critical role in determining the quality and uniformity of the NiS film deposited on the substrate. Notably, the use of nickel chloride resulted in the formation of a more uniform and continuous NiS layer (Fig. 1b). In contrast, films synthesized using nickel sulfate, acetate, and nitrate exhibited noticeable cracking and inhomogeneities, suggesting that these salts lead to less favorable deposition characteristics under the given conditions (Fig. 1a,c,d). The observed cracking in NiS layers synthesized from nickel sulfate, acetate, and nitrate precursors can be attributed to several factors. These salts likely promote less controlled or uneven nucleation and growth of the NiS layer during the SILAR process, resulting in internal stresses within the film. Additionally, highly hydrated anions such as sulfate and nitrate may alter the deposition kinetics, leading to rapid precipitation and structural inhomogeneities. Upon drying or crystallization, these stresses can manifest as cracks due to shrinkage and poor mechanical integrity. In contrast, the use of nickel chloride as the precursor yields a more uniform and compact NiS thin film, likely due to its lower degree of ion hydration and more favorable deposition behavior.

EDX spectrum data demonstrate presence of Ni, S, O and C atoms in synthesized nanolayers.

Figure 2(a) illustrates the FTIR spectra of nickel sulfides synthesized using NiSO<sub>4</sub>, NiCl<sub>2</sub>, NiAc<sub>2</sub> and Ni(NO<sub>3</sub>)<sub>2</sub>. Absorption bands characteristic of nickel sulfide with minor differences in intensity are observed in all spectra. Weak bands observed at about 3670 and 1640 cm<sup>-1</sup> are corresponding to valence and bending vibrations bonds of O–H bond in water molecules, respectively. Bands with peaks at 1080 and 2339 cm<sup>-1</sup> are correlated to CO<sub>2</sub>, which is thought to be adsorbed on the surface of samples from the atmosphere during sample preparation [17]. The peaks at 500, 555 and 670 cm<sup>-1</sup> could be assigned to bending vibration mode in Ni–S [18].

Figure 2(b) show the XRD pattern thin film of nickel sulfide obtained from nickel chloride precursor. It should be noted that a similar diffraction pattern was observed for sulfides obtained from other precursors. A single intense peak is observed with value  $33.7^{\circ}$  corresponding to lattice parameter (002), respectively, in agreement with standard data card (JCPDS: 12-0041) of NiS<sub>x</sub>. Peak with value  $62.1^{\circ}$  correspond to  $K_{\beta}$  of substrate.

The electrochemical performance of the NiS electrode was evaluated by cyclic voltammetry (CV) and galvanostatic charge discharge technology (GCD). Fig. 3(a) shows the CV curves of NiS electrodes synthesized using NiSO<sub>4</sub>, NiCl<sub>2</sub>, NiAc<sub>2</sub> and Ni(NO<sub>3</sub>)<sub>2</sub> on Ni foam after 10 SILAR cycles. The peaks present are related to typical redox peaks of Ni<sup>2+</sup> to Ni<sup>3+</sup> [19]. Probable reaction mechanism of these redox peaks may be related to the following eq. (2):

$$NiS + OH^{-} \rightleftharpoons NiSOH + e^{-}. \tag{2}$$

However, it can be noted that the Ni<sup>2+</sup> to Ni<sup>3+</sup> transition potential is different for each electrode. Moreover, the lowest potential at which this process occurs corresponds to nickel sulfide synthesized from nickel chloride. It can be hypothesized that the anions (such as sulfate, chloride, nitrate, etc.) exert an influence on the electrochemical behavior

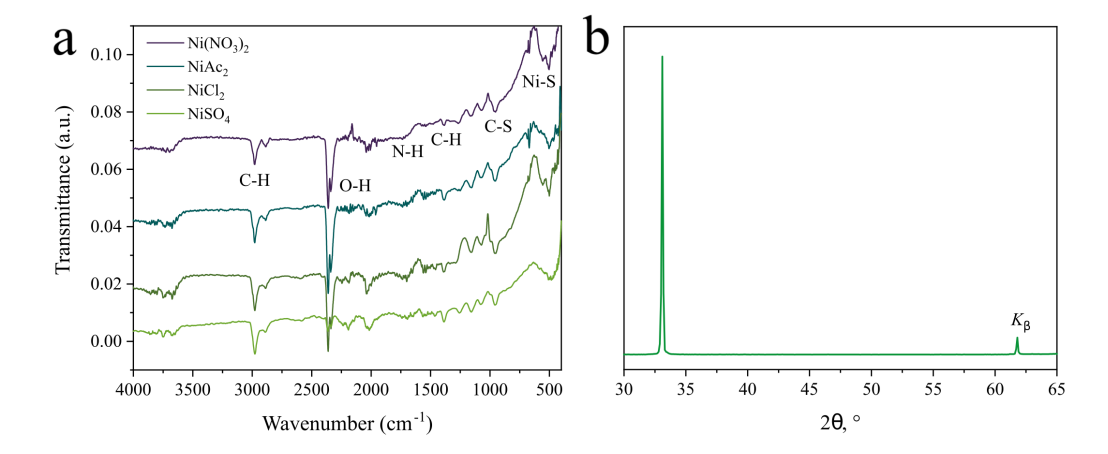


FIG. 2. (a) FTIR spectra of nickel sulfides synthesized using  $NiSO_4$ ,  $NiCl_2$ ,  $NiAc_2$  and  $Ni(NO_3)_2$  and (b) XRD pattern of nickel sulfides synthesized using  $NiCl_2$ 

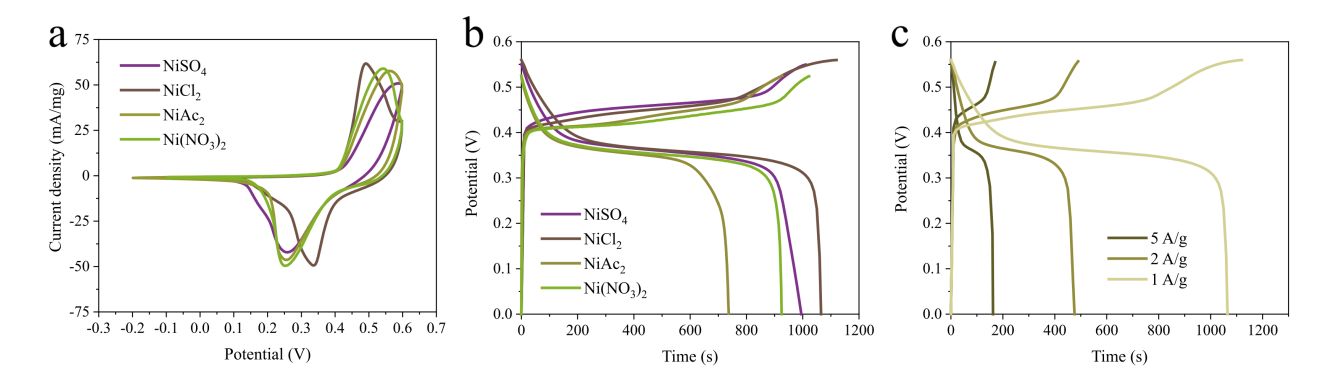


FIG. 3. (a) CV curves at scan rate of 10 mV/s and (b) GCD curves at current density of 1 A/g in 1 M KOH electrolyte of nickel sulfides synthesized using NiSO<sub>4</sub>, NiCl<sub>2</sub>, NiAc<sub>2</sub> and Ni(NO<sub>3</sub>)<sub>2</sub> on NF after 10 SILAR cycles, (c) GCD curves at different current density of nickel sulfide synthesized using NiCl<sub>2</sub> after 10 SILAR cycles

of nickel, potentially through the formation of surface complexes or modifications in the material's structural properties. These effects could lead to a shift in the oxidation/reduction peak potential, depending on the chemical nature and reactivity of the anions.

The galvanostatic charge-discharge curves of electrodes are shown in Fig. 3(b). The nonlinear shape of the curves indicates the pseudocapacitive properties of the electrodes. The specific capacitance values calculated from the charge-discharge curves at a current density of 1 A/g (Fig. 3b) for electrodes synthesized using NiSO<sub>4</sub>, NiCl<sub>2</sub>, NiAc<sub>2</sub> and Ni(NO<sub>3</sub>)<sub>2</sub> were 1809, 1902, 1401 and 1762 F/g, respectively. Thus, the sample synthesized from nickel chloride has the best capacitive characteristics. This enhanced electrochemical performance directly correlates with improved morphology electrode synthesized using NiCl<sub>2</sub>, as the continuous and crack-free structure facilitates better electron and ion transport, reduces charge transfer resistance, and ensures more effective utilization of electroactive sites. Consequently, the NiS layer derived from nickel chloride exhibits superior electrochemical properties compared to the more fractured and structurally defective layers obtained used other salts.

A comparative analysis of the electrochemical performance of the synthesized nickel sulfide with nickel sulfide-based electrodes obtained by other synthetic techniques is presented in Table 1. The results provide compelling evidence for the efficacy of the SILAR method as an effective approach for the synthesis of nickel sulfide. Furthermore, a detailed investigation into the influence of various synthesis conditions such as the choice of nickel salts and deposition parameters on the electrochemical properties of the resulting material has been conducted. These findings contribute to a deeper understanding of how synthesis conditions can be optimized to enhance the performance of nickel sulfide electrodes, highlighting the potential of this method for future applications in energy storage and conversion technologies.

TABLE 1. Comparative characteristics of electrodes based on nickel sulfide obtained by different synthetic techniques

Electrode	Substrate	Method	Specific capacitance (F/g)	Electrolyte	Stability	Ref
$\mathrm{NiS}_x$	Ni foam	SILAR	1902 at 1 A/g	1 M KOH	100 % after 1000 cycles	This article
Ni <sub>3</sub> S <sub>2</sub> (h-NS20)/Co <sub>3</sub> O <sub>4</sub>	Ni foam	SILAR	1901 at 1 A/g	1 M KOH	91.8 % after 10000 cycles	[20]
NiS/NiSSe nanosheet	Ni foam	hydrothermal technique	1908 at 1 A/g	PVA/KOH gel electrolyte	>90 % after 28000 cycles	[21]
NiS/ACNTs	Ni foam	hydrothermal method and subsequent annealing treatment	1266 at 1 A/g	3 М КОН	83 % after 2000 cycles	[22]
NiS NPs	Ni foam	hydrothermal method	1073.8 at 1.2 A/g	2 M KOH	89 % after 1000 cycles	[23]

#### 4. Conclusion

This study demonstrates the impact of nickel salt precursors on the morphology and electrochemical performance of nickel sulfide films synthesized via the SILAR method. Among the salts investigated, nickel chloride produced the most uniform and mechanically stable  $\mathrm{NiS}_x$  layer, free of visible cracks and defects. This improved film quality was found to be directly responsible for the superior electrochemical performance, with the chloride-derived  $\mathrm{NiS}_x$  electrode achieving a specific capacitance of 1902 F/g at 1 A/g. In contrast, layers formed from nickel sulfate, acetate, and nitrate exhibited significant cracking, which negatively affected charge transport and capacitance. The results underscore the importance of precursor selection in controlling the microstructure and optimizing the electrochemical properties of nickel sulfide-based electrodes, offering valuable insights for the development of advanced materials for supercapacitor and energy storage technologies.

## References

- [1] Lakshmi K.C.S., Vedhanarayanan B. High-performance supercapacitors: a comprehensive review on paradigm shift of conventional energy storage devices. *Batteries*, 2023, **9** (4), P. 202–247.
- [2] Shariq M., Alhashmialameer D., Adawi H., Alrahili M.R., Almashnowi M.Y.A., Alzahrani A., Sharma M., Ali S.K., Slimani Y. Advancements in transition metal sulfide supercapacitors: a focused review on high-performance energy storage. *J. Ind. Eng. Chem.*, 2025, **144**, P. 269–291.
- [3] Gao Y., Zhao L. Review on recent advances in nanostructured transition-metal-sulfide-based electrode materials for cathode materials of asymmetric supercapacitors. CEJ, 2022, 430 (2), 132745.
- [4] Guan Y., Hu K., Su N., Zhang G., Han Y., An M. Review of NiS-based electrode nanomaterials for supercapacitors. *Nanomaterials*, 2023, 13 (6), P. 979–1014.
- [5] Pothu R., Bolagam R., Wang Q.H., Ni W., Cai J.F., Peng X.X., Feng Y.Z., Ma J.M. Nickel sulfide-based energy storage materials for high-performance electrochemical capacitors. *Rare Met.*, 2021, **40**, P. 353–373.
- [6] Yan H., Zhu K., Liu X., Wang Y., Wang Y., Zhang D., Lu Y., Peng T., Liu Y., Luo Y. Ultra-thin NiS nanosheets as advanced electrode for high energy density supercapacitors. *RSC Adv.*, 2020, **10**, P. 8760–8765.
- [7] Gou J., Xie S., Yang Z., Liu Y., Chen Y., Liu Y., Liu C. A high-performance supercapacitor electrode material based on NiS/Ni<sub>3</sub>S<sub>4</sub> composite. Electrochim. Acta, 2017, 229, P. 299–305.
- [8] Parveen N., Ansari S.A., Ansari S.G., Fouad H., El-Salam N.M.A., Cho M.H. Solid-state symmetrical supercapacitor based on hierarchical flower-like nickel sulfide with shape-controlled morphological evolution. *Electrochim. Acta*, 2018, **268**, P. 82–93.
- [9] Chen X., Sun M., Jaber F., Nezhad E.Z., Hui K.S, Li Z., Bae S., Ding M. A flexible wearable self-supporting hybrid supercapacitor device based on hierarchical nickel cobalt sulfide@C electrode. *Sci Rep.*, 2023, 13, 15555.
- [10] Patil A.M., Lokhande V.C., Lokhande A.C., Chodankar N.R., Ji T., Kim J.H., Lokhande C.D. Ultrathin nickel sulfide nano-flames as an electrode for high performance supercapacitor; comparison of symmetric FSS-SCs and electrochemical SCs device. RSC Adv., 2016, 6, P. 68388–68401.
- [11] Yu L., Yang B., Liu Q., Liu J., Wang X., Song D., Wang J., Jing X. Interconnected NiS nanosheets supported by nickel foam: soaking fabrication and supercapacitors application. *J. Electroanal. Chem.*, 2015, **739**, P. 156–163.
- [12] Ratnayake S.P., Ren J., Colusso E., Guglielmi M., Martucci A., Gaspera E.D. SILAR deposition of metal oxide nanostructured films. *Small*, 2021, 2101666.
- [13] Lobinsky A.A., Kodintsev I.A., Tenevich M.I., Popkov V.I. A novel oxidation–reduction route for the morphology-controlled synthesis of manganese oxide nanocoating as highly effective material for pseudocapacitors. *Coatings*, 2023, **13** (2), 361.
- [14] Lobinsky A.A., Kaneva M.V., Tenevich M.I., Vadim Popkov V.I., Direct Synthesis of Mn<sub>3</sub>[Fe(CN)<sub>6</sub>]<sub>2</sub> · nH<sub>2</sub>O Nanosheets as Novel 2D Analog of Prussian Blue and Material for High-Performance Metal-Ion Batteries. *Micromachines*, 2023, **14** (5), 1083.
- [15] Zhang F., Ouyang R., Zhou T., Xiong C., Shi W., Su X., Zeng T., Chen Y., Dong G. The effect of different anions on the crystallization course of α-Al<sub>2</sub>O<sub>3</sub> powder in hydrothermal method. *App. Cer. Tech.*, 2024, **21** (3), P. 1450–1460.

- [16] Matussin S.N., Rahman A., Khan M.M. Role of Anions in the Synthesis and Crystal Growth of Selected Semiconductors. Front. Chem., 2022, 10, 881518
- [17] Khan N.A., Rashid N., Junaid M., Zafar M.N., Faheem M., Ahmad I. NiO/NiS Heterostructures: An Efficient and Stable Electrocatalyst for Oxygen Evolution Reaction. ACS Applied Energy Materials, 2019, 2 (5), P. 3587–3594.
- [18] Nachimuthu S., Kannan K., Thangavel S., Gurushankar K. Electrochemical and magnetic properties of 3D porous NiS/CuS nanocomposites. Applied Surface Science Advances, 2022, 7, 100209.
- [19] Liu H., Liu X.-J., Dong F.-Y., Sun X.-Z. A direct-write method for preparing a bimetal sulfide/graphene composite as a free-standing electrode for high-performance microsupercapacitors. RSC Advances, 2020, 10, 35490.
- [20] Mishra D., Kim S.Y., Jin S.H. Hierarchically-Formed Nickel Sulfide Heterostructure via SILAR on Hydrothermally Grown Cobalt Oxide Scaffolds: Role of Number of Over-Coating and Evolution of Electrochemical Performance in Supercapacitor Electrodes. *Applied Surface Science*, 2021, 564 (4), 150436.
- [21] Charis C., Batabyal S.K., Pramana S.S., Das B. Nickel sulfide-nickel sulfoselenide nanosheets as a potential electrode material for high performance supercapacitor with extended shelf life. *J. of Energy Storage*, 2023, **68**.
- [22] Ouyang Y., Chen Y., Peng J., Yang J., Wu C., Chang B., Guo X., Chen., Luo Z., Wang X. Nickel sulfide/activated carbon nanotubes nanocomposites as advanced electrode of high-performance aqueous asymmetric supercapacitors. *J. of Alloys and Compounds*, 2021, **885**, 160979.
- [23] Bandari N., Punnoose D., Rao S.S., Subramabnian A., Ramesh B.R., Kim H.-J. Hydrothermal synthesis and pseudocapacitive properties of morphology-tuned nickel sulfide (NiS) nanostructures. New J. Chem., 2018, 42, P. 2733–2742.

Submitted 21 August 2025; accepted 26 August 2025

Information about the authors:

*Maria V. Kaneva* – Ioffe Institute, Hydrogen Energy Laboratory, St Petersburg, 194021, Russia; ORCID 0000-0003-2816-7059; skt94@bk.ru

*Alexandra A. Meleshko* – Ioffe Institute, Hydrogen Energy Laboratory, St Petersburg, 194021, Russia; ORCID 0000-0002-7010-5209; alya\_him@mail.ru

Maxim I. Tenevich – Ioffe Institute, Hydrogen Energy Laboratory, St Petersburg, 194021, Russia; ORCID 0000-0003-2003-0672; mtenevich@gmail.com

*Maria O. Enikeeva* – Ioffe Institute, Hydrogen Energy Laboratory, St Petersburg, 194021, Russia; ORCID 0000-0002-9633-4421; enikeeva123@mail.ioffe.ru

Ilya A. Kodintsev – Ioffe Institute, Hydrogen Energy Laboratory, St Petersburg, 194021, Russia; i.a.kod@mail.ru

Artem A. Lobinsky – Ioffe Institute, Hydrogen Energy Laboratory, St Petersburg, 194021, Russia; ORCID 0000-0001-5930-2087; lobinski.a@mail.ru

Conflict of interest: the authors declare no conflict of interest.